



HAL
open science

Investigating the relationship between cranial bone thickness and diploic channels: A first comparison between fossil *Homo sapiens* and *Homo neanderthalensis*

Jiaming Hui, Antoine Balzeau

► To cite this version:

Jiaming Hui, Antoine Balzeau. Investigating the relationship between cranial bone thickness and diploic channels: A first comparison between fossil *Homo sapiens* and *Homo neanderthalensis*. *The Anatomical Record: Advances in Integrative Anatomy and Evolutionary Biology*, 2023, 10.1002/ar.25360 . hal-04336005

HAL Id: hal-04336005


<https://hal.sorbonne-universite.fr/hal-04336005>

Submitted on 11 Dec 2023

HAL is a multi-disciplinary open access archive for the deposit and dissemination of scientific research documents, whether they are published or not. The documents may come from teaching and research institutions in France or abroad, or from public or private research centers.

L'archive ouverte pluridisciplinaire **HAL**, est destinée au dépôt et à la diffusion de documents scientifiques de niveau recherche, publiés ou non, émanant des établissements d'enseignement et de recherche français ou étrangers, des laboratoires publics ou privés.

Investigating the relationship between cranial bone thickness and diploic channels: A first comparison between fossil *Homo sapiens* and *Homo neanderthalensis*

Jiaming Hui^{1,2}  | Antoine Balzeau^{1,3}

¹PaleoFED Team, UMR 7194 Histoire Naturelle de l'Homme Préhistorique, CNRS, Département Homme et Environnement, Muséum national d'Histoire naturelle, Paris, France

²Ecole Doctorale 227 Sciences de la nature et de l'Homme: évolution et écologie, Sorbonne Université, Paris, France

³Department of African Zoology, Royal Museum for Central Africa, Tervuren, Belgium

Correspondence

Jiaming Hui, UMR 7194 Histoire Naturelle de l'Homme Préhistorique, Muséum national d'Histoire naturelle, 17 place du Trocadéro, Paris 75016, France.
Email: jiaming.hui@etu.sorbonne-universite.fr

Funding information

Agence Nationale de la Recherche, Grant/Award Number: ANR-20-CE27-0009; China Scholarship Council

Abstract

Diploic veins are part of the circulatory system of the head. They transport venous blood and cerebrospinal fluid and are housed in diploic channels (DCs). DCs are highly variable in terms of their position, extension, and size. These parameters were hypothesized to be related to the variations in cranial vault thickness (CVT). For the first time, we analyzed the spatial relationship between CVT and DCs in a sample of eight *H. neanderthalensis* and *H. sapiens* cranial fossils. Using micro-CT scanning data, we constructed color maps of the CVT and visually inspected whether the regional thickness variation was associated with the morphology and distribution of the DC branches. The results showed that when regional bone thickness was below a certain threshold, no DCs or scattered small DC branches were present. Larger DC branches appeared only when the thickness exceeded the threshold. However, once the threshold was reached, further increases in thickness no longer resulted in more or larger DCs. This study also found that our sample of *H. neanderthalensis* and *H. sapiens* have different distribution patterns in thin areas, which may affect how their DCs connect with different branches of the middle meningeal vessels. This preliminary study provides evidence for the discussion on the interaction between the cranium, brain, and blood vessels. Future research should include more hominin fossils to better document the variation within each species and possible evolutionary trends among hominin lineages.

KEYWORDS

bone thickness, diploic veins, internal cranial anatomy, original fossils, virtual anthropology

1 | INTRODUCTION

The diploic channels (DCs) course between the compact layers of the cranial bones, bridging the extracranial and intracranial vascular networks (Breschet, 1829; García-González et al., 2009; Hershkovitz et al., 1999; Lachkar

et al., 2019). DCs play an important role in the transport of venous blood and cerebrospinal fluid (Tsutsumi et al., 2015, 2014; Yamashiro et al., 2021). Previous studies have hypothesized that DCs are associated with brain evolution because they are involved in brain metabolism and heat management (Falk, 1990; Kunz & Iliadis, 2007;

This is an open access article under the terms of the [Creative Commons Attribution](https://creativecommons.org/licenses/by/4.0/) License, which permits use, distribution and reproduction in any medium, provided the original work is properly cited.

© 2023 The Authors. *The Anatomical Record* published by Wiley Periodicals LLC on behalf of American Association for Anatomy.

Rangel de Lázaro et al., 2016, 2020). Thus, identifying the evolutionary trajectory and variable morphology of DCs across hominin specimens should provide a better understanding of the interaction between the brain and cranial circulatory system during human evolution.

Although there are limited studies on DCs, most have noted high variability in this vascular network (García-González et al., 2009; Hershkovitz et al., 1999; Rangel de Lázaro et al., 2020; Tsutsumi et al., 2013). However, the factors associated with the variations in DCs remain unclear. A possible factor frequently discussed is the cranial vault thickness (CVT) (Eisová et al., 2016; Rangel de Lázaro et al., 2020). The cranial bones provide space for DC extension. Thicker bones allow for expansion of the DC system in terms of both size and complexity. Concurrently, the morphology of DCs can influence the blood flow volume and drainage pathways in the bones where they run, which may affect bone mineralization, maturation, and metabolism (Eisová et al., 2016; Marks & Odgren, 2002; Percival & Richtsmeier, 2013). Therefore, thicker bones may require adaptations to the DC system.

Hershkovitz et al. (1999) compared two groups of extant adult humans with developed and undeveloped DC systems and showed that the developed group had slightly thinner midfrontal regions and slightly thicker mid parietal regions. Eisová et al. (2016) tested the relationship between parietal CVT and DC diameter in extant human populations and found no patent correlation between them. In contrast, Rangel de Lázaro et al. (2020) studied the growth rates of DCs and cranial bones in dry skulls with estimated age ranges (including non-adults) and found that CVT was a major determinant of DC morphology, although the growth rates of DCs and cranial bones were different. Rangel de Lázaro et al. (2020) hypothesized that CVT was a threshold factor. In other words, the DC system can develop only after the bones have reached their minimum thickness.

Current evidence is insufficient to determine whether there is a correlation between DC systems and CVT. In addition, previous studies measured the average thickness of entire bones, although we know that each cranial vault bone varies in thickness across its area. We do not yet know whether uneven thickness distribution within a cranium influences the spatial distribution of DCs, and if so, how. Furthermore, hominin species exhibit various CVT distribution patterns (Balzeau, 2007, 2013; Beaudet et al., 2018; Gauld, 1996). We hypothesize that if CVT is a major determinant of DC morphology, hominin species would vary in their DC systems, which could reflect variations in the configuration of the cranial circulatory system.

We test these ideas by comparing *Homo neanderthalensis* with the fossil *Homo sapiens*. *H. neanderthalensis* is

characterized by an abundance of cranial fossil remains, many of which have well-preserved diploic layers. The size of the samples and preservation of the diploe are important for collecting adequate data to test the hypotheses about DC morphology, its relationship with CVT, and to allow comparison with *H. sapiens*. Additionally, *H. neanderthalensis* has a similar brain size to *H. sapiens* (Aiello & Dean, 1990; Schwartz et al., 2002). This allows us to minimize the influence of cranial size, which is another factor hypothesized to be associated with the morphology of the DC system (Eisová et al., 2016, 2022; Hershkovitz et al., 1999; Rangel de Lázaro et al., 2020). Therefore, the present study compares the distribution patterns of CVT and the relationships between local CVT and DC systems in several key *H. neanderthalensis* and *H. sapiens* fossils. The aims of this study are to (1) determine whether the regional thickness of the cranium is related to the distribution and morphology of the DC system and (2) explore whether the differences in the DC system between our sample of *H. neanderthalensis* and fossil *H. sapiens* are related to their distinct distribution patterns of the CVT.

2 | MATERIALS AND METHODS

Our samples comprised four *H. neanderthalensis* and four *H. sapiens* cranial fossils (Table 1). Fossil specimens were discovered in Western Europe and curated at the French National Natural History Museum and Royal Belgian Institute of Natural Sciences. All fossils date back to the Late Pleistocene (Devièse et al., 2021; Douka et al., 2020; Henry-Gambier, 2002; Raynal & Pautrat, 1990; Semal et al., 2009), and are relatively well preserved. The microtomography platform “RX Solutions EasyTom 150” was applied to scanning the Spy 1 and Spy 10 crania, and the platform “Phoenix V|tome|x L240” was used to scan all other crania (Hui & Balzeau, 2023). The voxel thicknesses of all the Micro-CT images of the sample were below 0.15 mm, which allowed the reconstruction of even the microscopic structures.

In this study, we used the 3D models of DCs from our previously published work (Hui & Balzeau, 2023), in which we detailed the criteria for identifying DCs and the protocols for 3D modeling. In this previously published work, the DCs were identified by visually inspecting the micro-CT images and translucent 3D models of fossil crania using the software 3D Slicer v4.13 (Fedorov et al., 2012). If visual inspections revealed a structure in the diploe with a vascular-like shape and connections with other vessels or DCs, we classified this structure as a DC. The 3D modeling of DCs in the previous study was conducted continually in 3D Slicer (Hui & Balzeau, 2023).

TABLE 1 The inventory of the materials.

Species	Specimen	Locality	Material source
<i>H. sapiens</i>	Cro-Magnon 1	Dordogne, France	MH
	Cro-Magnon 2	Dordogne, France	MH
	Cro-Magnon 3	Dordogne, France	MH
	Abri-Pataud	Dordogne, France	MH
<i>H. neanderthalensis</i>	La Chapelle-aux-Saints 1	Corrèze, France	MH
	La Quina H5	Charente, France	MH
	Spy 1	Namur, Belgium	RBINS
	Spy 10	Namur, Belgium	RBINS

Abbreviations: MH, Musée de l'Homme (a department of the French National Natural History Museum), Paris, France; RBINS, Royal Belgian Institute of Natural Sciences, Brussels, Belgium.

For most DC branches, the gray levels of their voxels were distinct from those of the surrounding bones. Thus, the “Flood filling” function in the software could distinguish those DCs from the bone and automatically conduct the segmentation in this previous study. Still, the gray levels of a few branches were similar with those of bones, and we in this previous study used the “Paint” function to segment these branches manually. After segmentation, the 3D Slicer automatically displayed the DC models as three-dimensional visualizations.

Through qualitative inspection, we in this current study estimated the distribution, pathway, amount, and size of DC branches in the crania. Like in the previous study (Hui & Balzeau, 2023), a DC with more offshoots and longer pathway and diameter was considered “more developed” in our subsequent qualitative descriptions. Conversely, a DC branch could be described as “narrow” or “small” if qualitative inspection found its diameter or length to be shorter than those of the majority of DC networks.

This study was also able to reconstruct 3D models of both the endocasts and external surfaces of the crania using 3D Slicer. We then used the “Surface distance” function of Avizo v9.0 (FEI, Hillsboro, Oregon) to estimate the distances between the endocast and external surface. For the neurocranium, this distance is equal to the bone thickness (i.e., CVT). The “Surface Distance” function automatically generated 3D color maps, in which the color representing distance values ranged from light blue (lower) to yellow (higher). By referring to the color scale, we estimated the local values of the neurocranium. This study was limited to the frontal, parietal, and occipital bones, where DCs are usually distributed. Additionally, as in some specimens, the thicknesses of some regions were distorted by the artificial filling materials, and these affected regions were excluded from the color map.

For comparison, we used a color scale ranging between 2 and 22 mm for all specimens. Lowering the

lower limit to 2 mm ensured that the most extremely thin regions could be included within the analysis range. To cover the thickest part of the neurocranium (the supraorbital ridge and frontal crest), the upper limit was raised to 22 mm. Regions with distance values <2 mm were uniformly shown in white, whereas regions with distance values >22 mm were uniformly shown in yellow. Thus, the facial parts (except the supraorbital ridge) that had high values were all displayed in yellow and were excluded from the analysis. For our specimens, this scale (2–22 mm) was sufficient to show the details of the variation in the neurocranial CVT. Additionally, as this scale has been applied in many studies (Balzeau, 2013; Balzeau et al., 2017; Balzeau & Charlier, 2016), using a unified scale would benefit future comparisons among independent studies.

Finally, we qualitatively compared the general thickness of each bone to the size and amount. We also identified the relatively thin and thick areas within each bone to estimate the spatial relationship between these areas and the DC network. Statistical analysis was not possible because of the sample size and variable completeness of the specimens.

3 | RESULTS

3.1 | *Homo sapiens*

3.1.1 | Cro-Magnon 1

The thickest area of the frontal bone is the supraorbital ridge (ranges from 14.5 to 21.5 mm), which houses many narrow DCs (Figures 1 and 2). Most of the frontal DC network is housed in the thick frontal squama. The upper part (5.0–15.5 mm) of the frontal squama is thicker than the lower part (7.5–12.5 mm), but the upper part does not display more DC branches. The lower part of the

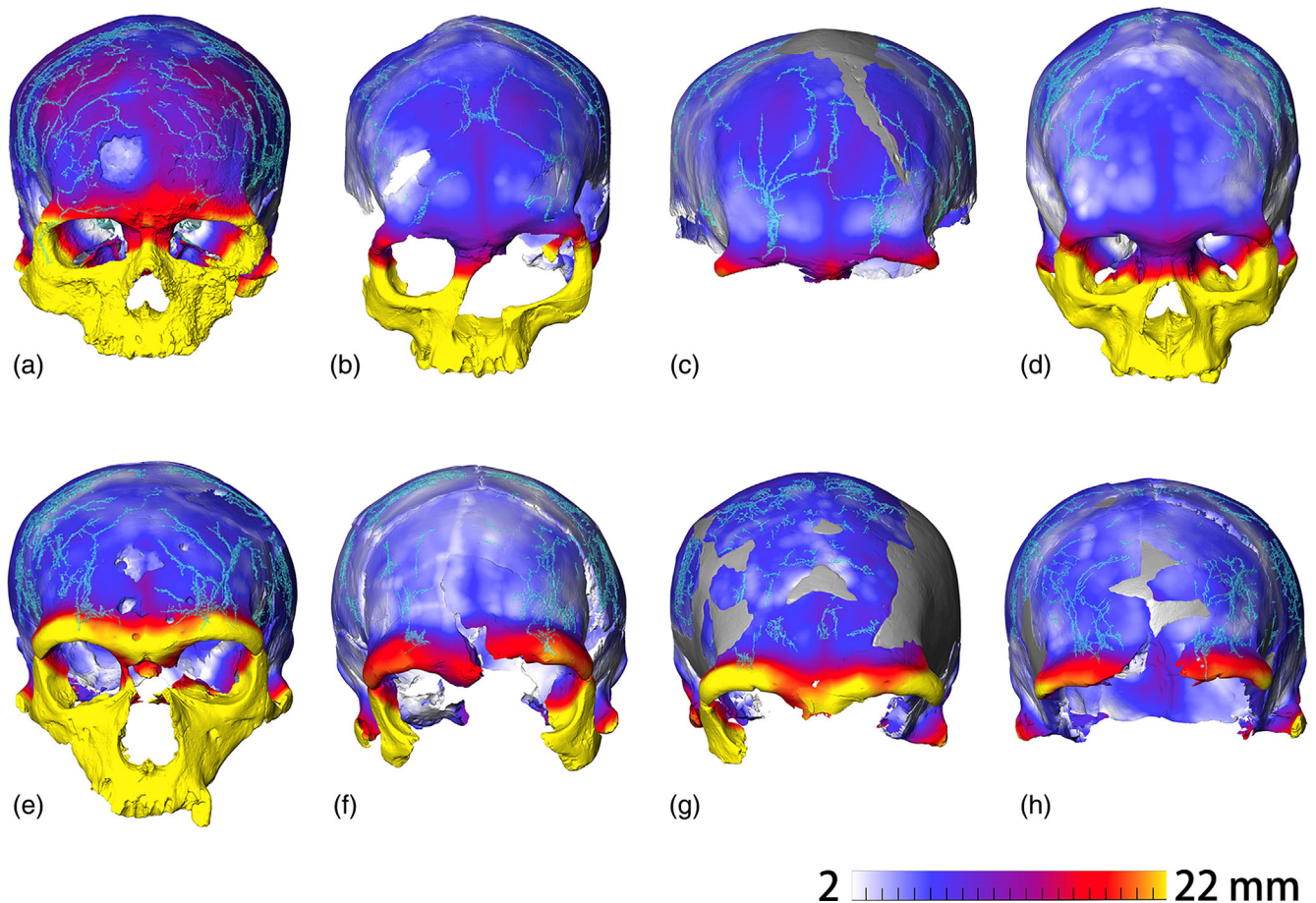


FIGURE 1 The anterior views of the DCs and surface-distance color maps. (a–d) Cro-Magnon 1, Cro-Magnon 2, Cro-Magnon 3, and Abri Pataud; (e–h) La Chapelle-aux-Saints 1, La Quina H5, Spy 1, and Spy 10. The areas affected by artificial filling materials are excluded and marked in gray. DCs, diploic channels.

temporal fossa of the frontal bone is very thin (2.0–5.0 mm) and there are no DC (Figure 3). A pathological area exists in the frontal squama where the diploic layer has been damaged; thus, we cannot judge whether any DCs ever existed there. However, the surrounding DC branches do not show a tendency to enter pathological areas. The thickness of the parietal bones is generally comparable to that of the frontal squama, which have numerous DCs. The upper third of the parietal bones is the thickest portion (4.5–14.5 mm), but the DCs are not relatively more developed in this area. In the bregmatic area and the lower third of the parietal bones (adjacent to the squamosal suture), there are relatively thin areas (<4.5 mm). The main DC branches bypass these thin areas and only a few narrow DCs extend to their edges. The occipital bone is generally thinner than the parietal and frontal bones, and displays a less developed DC network (Figures 3 and 4). Most occipital DCs are located along the midline, which is the thickest area (7.5–13.5 mm) of the occipital bone, although narrow DC branches also present in the relatively thinner areas (6.0–9.0 mm).

3.1.2 | Cro-Magnon 2

The supraorbital ridge (ranges from 9.0 to 14.0 mm) and frontal crest (9.5–11.5 mm) are the thickest areas of the frontal bone, but there are no DC in either area (Figures 1 and 2). The majority of the frontal DC network is distributed in the middle and upper frontal squama. Unlike Cro-Magnon 1, the most abundant area of DCs is adjacent to, but not in, the thickened area of the frontal squama (the center of the squama, ranges from 7.5 to 11 mm). Interestingly, we find that the bone is relatively thin (<4.5 mm) on both sides of the temporal line (Figure 3), while the temporal line itself is thicker (5.0–8.5 mm). In this area, the DCs course only along and beneath the temporal line, bypassing the relatively thin areas on both sides. The parietal bones are similar in thickness to the frontal squama and have comparably developed DC networks. Most parietal DCs are restricted to the relatively thick upper part (6.0–10.0 mm). They extend in the superoinferior direction and stop when approaching the boundary of the thin areas of the bone

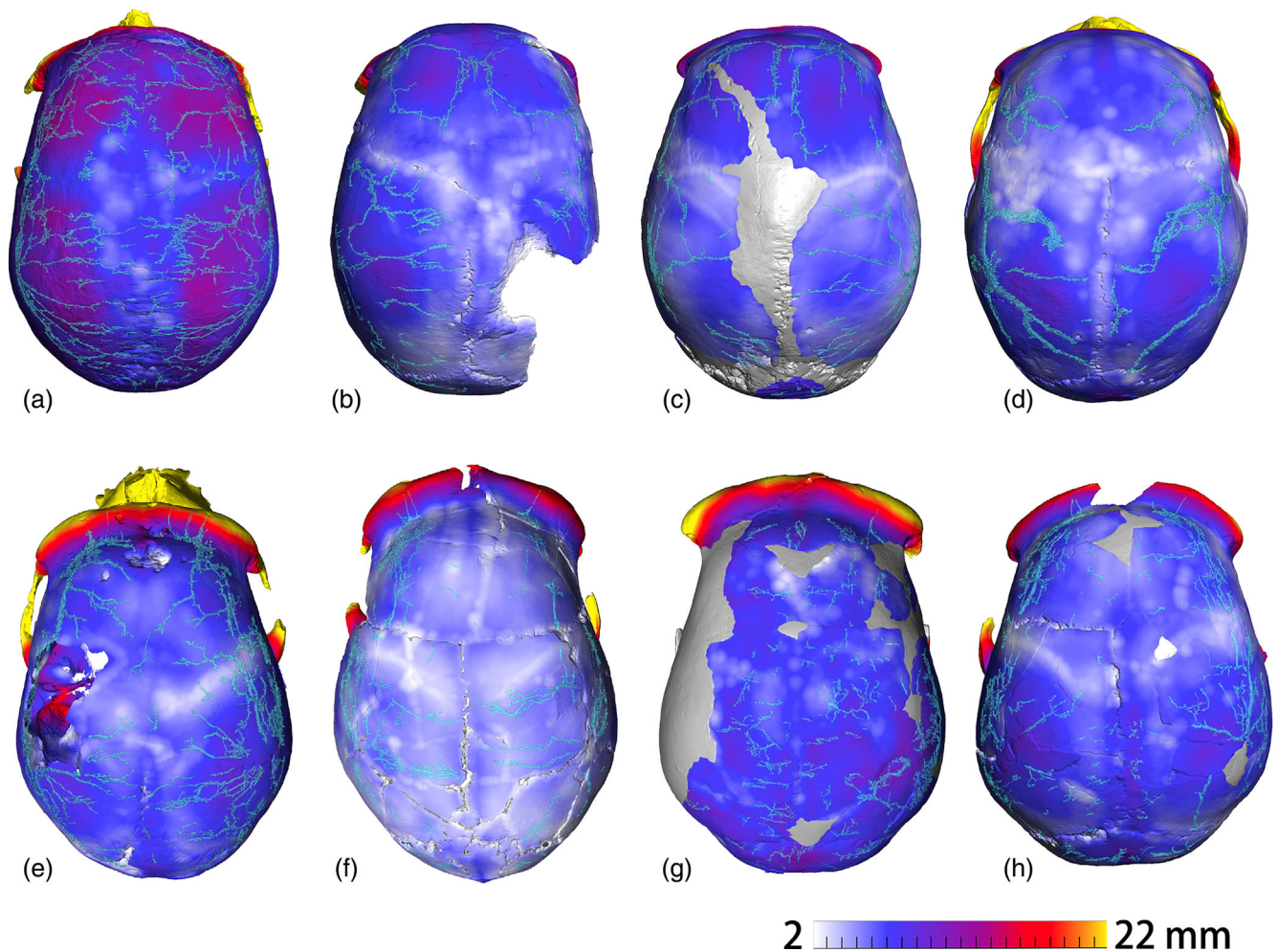


FIGURE 2 The superior views of the DCs and surface-distance color maps. (a–d) Cro-Magnon 1, Cro-Magnon 2, Cro-Magnon 3, and Abri Pataud; (e–h) La Chapelle-aux-Saints 1, La Quina H5, Spy 1, and Spy 10. The areas affected by artificial filling materials are excluded and marked in gray. DCs, diploic channels.

(3.0–6.0 mm), which correspond to the anterosuperior and lower parts of the parietal bone. The thickest areas of the parietal bones are located above the parietal eminence, reaching a maximum of 10.0 mm; they do not display the most abundant DCs. The DCs in the occipital bone are restricted in the relatively thick paralamdoid areas (5.5–7.0 mm) and the groove of the transverse sinus (5.0–10.5 mm, Figures 3 and 4). The extension of the occipital DCs stops before entering the thinnest area (3.0–3.5 mm) located in the cerebral fossa.

3.1.3 | Cro-Magnon 3

The thickest area of the frontal bone is the supraorbital ridge (ranges from 11.0 to 17.0 mm), where only a few narrow DCs pass through (Figures 1 and 2). The lower edge of the frontal squama (5.0–7.0 mm) houses rich DC branches and it is considerably thinner than the adjacent

supraorbital ridge. The most long and wide DC branches are distributed in the thicker areas of the frontal squama, whereas the thickest areas (peak at 10.0 mm) did not possess the most abundant branches. The thinnest area (<3.0 mm) of the frontal bone is located below the temporal line and shows no DC branches (Figure 3). There is an apparent difference in thickness between the two sides of the coronal suture. The anterior side (located on the frontal bone, 4.0–6.5 mm) is thicker, while the posterior side (located on the parietal bone, 3.0–5.5 mm) is thinner. In general, the entire paracoronary region contains only scarce DCs. The preserved part of the parietal bone is thinner than that of the frontal bone. The upper part of the parietal bones (3.5–8.0 mm) is slightly thicker than the lower (2.0–7.0 mm), but they both house comparable DC networks. The thinnest areas of the parietal bones correspond to the groove of the middle meningeal vessels (3.0–5.0 mm) and the area above the middle squamosal suture (2.0–3.5 mm). The latter does not exhibit DVs.

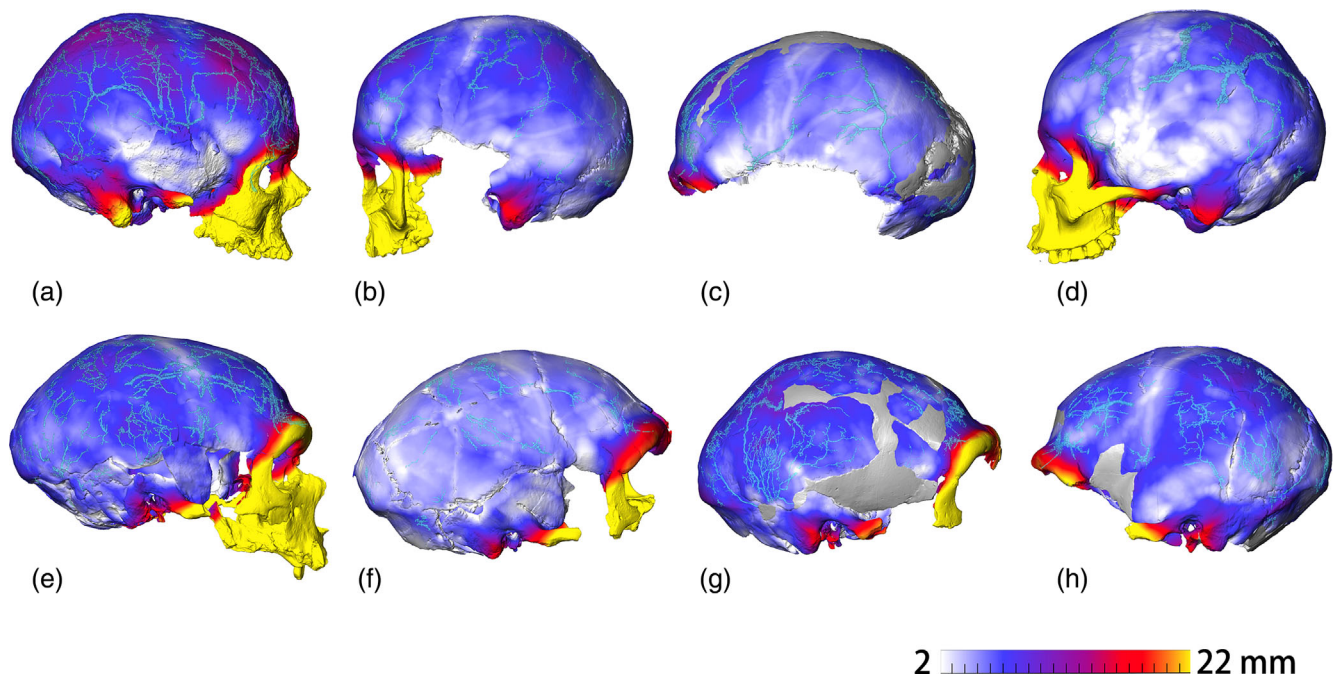


FIGURE 3 The lateral views of the DCs and surface-distance color maps. (a–d) Cro-Magnon 1, Cro-Magnon 2, Cro-Magnon 3, and Abri Pataud; (e–h) La Chapelle-aux-Saints 1, La Quina H5, Spy 1, and Spy 10. The better-preserved side of each specimen is presented. The areas affected by artificial filling materials are excluded and marked in gray. DCs, diploic channels.

In the preserved part of the occipital bone, most DCs are distributed along the midline (6.5–10.5 mm) and the groove of the transverse sinus (5.5–9.0 mm), which are the thickest areas (Figures 3 and 4). The extension of DC branches stops when approaching the edge of the thinner areas (3.5–4.5 mm) in the cerebral fossa.

3.1.4 | Abri-Pataud

The thickest areas of the frontal bone are the supraorbital ridge (9.0–13.0 mm) and the frontal crest (8.0–9.5 mm), where there are no DC branches (Figures 1 and 2). The frontal DCs bypass the thick center of the frontal squama (5.0–8.5 mm) and concentrate in the lateral part of the frontal bone (4.0–7.0 mm). In addition, frontal DCs bypass the thinnest area (<3.5 mm) located below the temporal line (Figure 3). The parietal bones are generally thicker than the frontal squama and house wider and longer DC branches. The sagittal suture (3.5–6.0 mm) and the anterior (<5.5 mm) and inferoposterior (<4.0 mm) parts of the parietal bones are the thinnest areas. Parietal DCs extend only to the boundaries of these thin areas without entering. The thickest area (peaks at 10.5 mm) of the parietal bone is located above the parietal eminence; however, it does not contain the most abundant branches. The thickness of the occipital bone is comparable to that of the parietal bone; however, only few DCs are observed in the occipital bone (Figures 3 and 4). The cerebral fossa

(4.0–6.0 mm) is thin and has no DCs. The occipital DCs are distributed along the groove of the transverse sinus (including the confluence of sinuses, 6.0–12.5 mm), which is the thickest area of the occipital bone.

In general, the thinning of the temporal fossa and the anterosuperior and inferior parts of the parietal bone was observed in the *H. sapiens* sample. A lack of DC branches in these relatively thin areas is also observed among *H. sapiens* specimens. In addition, the thinning and lack of DCs in the cerebral fossa is a pattern shared by Cro-Magnon 2, 3, and Abri-Pataud.

3.2 | *Homo neanderthalensis*

3.2.1 | La Chapelle-aux-Saints 1

The supraorbital ridge (>14.0 mm) is the thickest area of the frontal bone and contains many narrow DCs (Figures 1 and 2). The entire frontal squama is also a thick area (5.5–14.0 mm), compared with other areas in the whole neurocranium, and contains abundant large DC branches. The thinnest areas (<4.5 mm) of the frontal bone are located below the temporal line and no DCs are found (Figure 3). The overall thickness of the parietal bone is similar to that of the frontal squama and has a highly developed DC network. The thickest regions of the parietal bones have a rich network of DCs—they are the central area of the parietal bone (7.5–9.5 mm), the

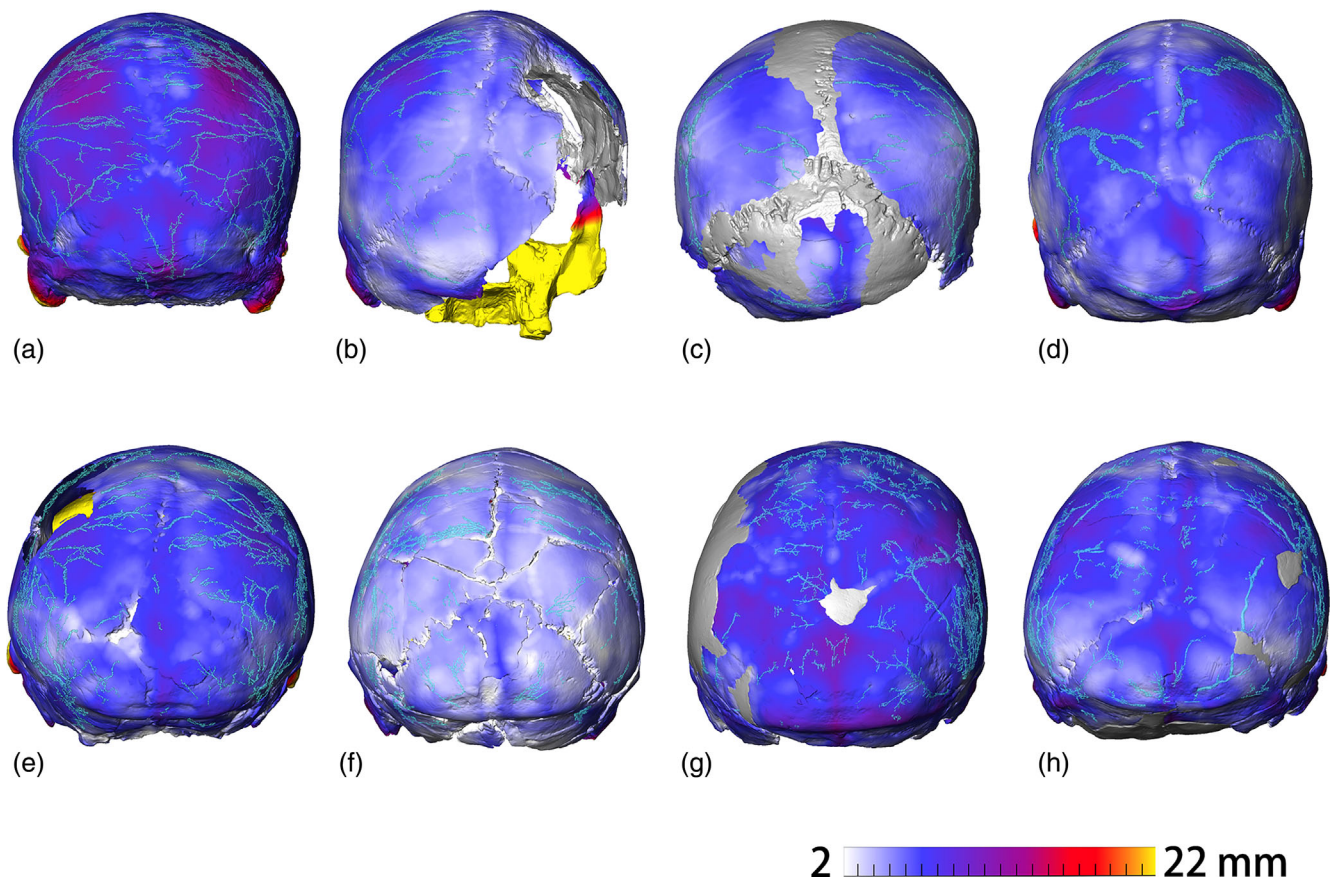


FIGURE 4 The posterior views of the DCs and surface-distance color maps. (a–d) Cro-Magnon 1, Cro-Magnon 2, Cro-Magnon 3, and Abri Pataud; (e–h) La Chapelle-aux-Saints 1, La Quina H5, Spy 1, and Spy 10. The areas affected by artificial filling materials are excluded and marked in gray. DCs, diploic channels.

areas near the lambdoid (6.5–9.0 mm), and the area above the squamosal suture (6.0–9.5 mm). The thinnest area of the parietal bone is the anterosuperior region (<4.0 mm), with only scattered small DC branches. The occipital bone is also thick, although fewer DCs are observed than in the frontal and parietal bones (Figures 3 and 4). Most occipital DCs are distributed in the cerebral fossa (5.0–7.5 mm) and the asterional region (5.0–9.0 mm), while there are only a few narrow DCs scattered along the midline (7.5–10.0 mm), which is the thickest part of the occipital bone.

3.2.2 | La Quina H5

The thickest part of the frontal bone is the supraorbital ridge (11.0–21.5 mm), where a few narrow DCs pass through (Figures 1 and 2). The general frontal squama is relatively thin, with the thinnest areas located below the temporal line (<3.0 mm, Figure 3) and at the center of the frontal squama (excluding the frontal crest, 3.0–5.5 mm). These thinnest areas display no DCs or only scattered narrow DCs. Most of the frontal DCs are

distributed in the lateral part of the frontal squama (3.5–7.5 mm), an area where thickness is slightly higher than the thinnest areas. The DCs and thicknesses of the parietal bones are comparable to those of the frontal squama. The thick areas of the parietal bone are the parasagittal (4.5–6.5 mm), central (4.0–6.5 mm), and lower (3.5–7.0 mm) regions, where the DCs are also mainly distributed. Thin areas (<4.0 mm) appear in the anterosuperior part of the parietal bone, where there is no distribution of large DC branches. The thickness of the occipital bone is similar to that of the parietal bone. However, there are fewer and smaller DCs in the occipital bone (Figures 3 and 4). While there are no main branches along the midline (5.0–8.0 mm), the thickest area, most of the occipital DCs are distributed in the relatively thinner asterional region (4.0–7.0 mm) and the cerebral fossa (3.5–6.0 mm).

3.2.3 | Spy 1

The thickest part of the frontal bone is the supraorbital ridge (>14.0 mm), which displays no DCs (Figures 1 and 2). The DCs in the frontal squama (4.5–14.0 mm) are

generally evenly distributed. The thinnest area (<4.5 mm) appears below the temporal line where there are no DC manifested (Figure 3). The thickness of the parietal bones is similar to that of the frontal squama; however, the parietal bones have a more developed network of DCs. The thickest areas of the parietal bones are in the central part (peak at 10.5 mm), but DCs are not the most abundant. The most developed DCs appear in the lower half of the parietal bones (5.5–7.5 mm). The thinnest area (5.5–7.0 mm) is located in the anterosuperior part of the parietal bones, where there are scattered narrow DCs. The thickness of the occipital bone was similar to that of the parietal bone; however, the occipital bone contains fewer and smaller DCs (Figures 3 and 4). There are a large number of DCs in the thickest area (9.5–11.5 mm) below the lambda, and there are also many branches distributed in the cerebral fossa (6.5–9.5 mm) and the asterional region (7.0–10.5 mm).

3.2.4 | Spy 10

The thickest area of the frontal bone is the supraorbital ridge (>10.0 mm); however, there are only a few DCs in this area (Figures 1 and 2). The frontal squama center (4.5–5.5 mm) and the two sides of the temporal line (4.0–6.0 mm) are thin and only have scattered DCs (Figures 2 and 3). In contrast, the other parts of the frontal squama are thicker (5.0–10.0 mm) and contain most of the large DC branches. The exception is the bregmatic area (6.5–8.0 mm), which is thick but does not display DCs. The parietal bones have a similar thickness and well-developed DC network as the frontal squama. The relatively thin areas of the parietal bone are located in the anterosuperior part (3.0–5.0 mm), the paralambdoid region (3.5–6.0 mm), and the asterional region (4.5–5.5 mm). The asterional region is rich in DCs, whereas the other thin areas have only a few narrow DCs. The center (5.5–10.0 mm) and parasagittal area (5.0–9.5 mm) of the parietal bone are thicker, and most of the DCs are distributed there. The thickest point (peak at 10.0 mm) of the parietal bone is at the center; however, DCs could not be observed because of taphonomic damage. The thickness of the occipital bone is similar to that of the parietal bone but with fewer and smaller DCs. The occipital DCs are mainly distributed in the midline (8.5–10.5 mm), the asterional region (6.5–10.5 mm), and the groove of the transverse sinus (4.5–9.0 mm), which are the thick areas (Figures 3 and 4). Additionally, some DCs extend into the edge of the relatively thin cerebral fossa (4.5–7.0 mm).

In comparison with the *H. sapiens* fossils (Figure 3), all *H. neanderthalensis* specimens also show thinning in

the temporal fossa of the frontal bone and the anterosuperior part of the parietal bone, where DC branches are absent or scarce. However, the inferior part of the parietal bone and cerebral fossa in most *H. neanderthalensis* specimens is relatively thick and possesses many DC branches, which is different from *H. sapiens* fossils.

4 | DISCUSSION

Our study presents a comparative analysis of CVT and DCs in samples of *H. neanderthalensis* and fossil *H. sapiens* to explore the potential relationship between CVT and DC distribution and morphology. Furthermore, we investigate whether the distinct CVT patterns of these two samples contributed to their DC characteristics.

Theoretically, there is an association between DC and CVT. Cranial vascular networks are involved in bone growth and metabolism (Eisová et al., 2016; Marks & Odgren, 2002; Percival & Richtsmeier, 2013). As DCs are part of the vascular system, a thicker cranial bone may require a more developed DC system for support. In addition, DCs may require a sufficiently thick bone to provide sufficient space for vascular extension. However, previous studies on the correlation between DC and CVT remain inconclusive, with contradictory findings (Eisová et al., 2016; Hershkovitz et al., 1999; Rangel de Lázaro et al., 2020).

Our samples of *H. sapiens* and *H. neanderthalensis* both exhibit a lack of DCs in relatively thin regions of the neurocranium. Notably, the DC branches from thicker areas terminate when approaching the edges of thin regions or circumvent them. However, outside these thin areas, CVT does not show an observable influence on the DCs. Specifically, regions with the highest CVT values, such as the supraorbital ridge, frontal crest, and the area above the parietal eminence, do not necessarily exhibit the highest density or largest diameter of DCs. In addition, when the frontal squama, parietal bone, and occipital bone have similar overall thicknesses, their DCs differ in both number and size. Notably, despite possessing an overall thickness comparable to that of the parietal bone, the occipital bone consistently has fewer and smaller DC branches.

Based on this evidence, it can be concluded that when the regional thickness is below a certain threshold, no DCs or scattered small DC branches are present. Larger DC branches appear only when the thickness exceeds a certain threshold. However, once the threshold is reached, further increases in bone thickness no longer result in more or larger DCs. This finding is consistent with the “threshold hypothesis” proposed in a previous study (Rangel de Lázaro et al., 2020), and it also explains

why previous statistical analyses find insignificant linear correlation between the DCs and CVT (Eisová et al., 2016). However, the threshold value varies among individuals. For instance, regions in the Cro-Magnon 1 cranium do not display DCs when the thinness falls below 4.5 mm. In contrast, in the Cro-Magnon 3 neurocranium, many large DC branches are in regions thinner than 4.5 mm, and the DCs only disappear when the local thickness decreases to approximately 3.5 mm. This may be related to the globally thinner vault in the latter than in the former. The threshold may be a specimen dependent in relation to the global thickness of the skull.

As previously explained, a more developed DC system may support a thicker cranial bone. However, it is important to note that the development and metabolism of cranial bones are supported by a complex network of vessels, both within and outside the skull, including the superficial temporal arteries, veins, middle meningeal vessels, and dural sinuses (Aiello & Dean, 1990; Grimaud-Hervé, 2002; Lang, 1983; Yu et al., 2016). Therefore, the cranial bones do not rely solely on DCs for nutritional or mechanical support.

Additionally, our study describes the characteristic distribution patterns of relatively thin regions of the neurocranium in *H. neanderthalensis* and fossil *H. sapiens*. Specimens of both species show relatively thin regions of frontal bone inferior to the temporal line. All specimens have a thin anterosuperior portion of the parietal bone. However, the specimens differ in the inferior portions of the parietal bone. The inferior portion of the parietal bone in our sample of *H. sapiens* demonstrated evident thinning, whereas the inferior portion of the parietal bone in *H. neanderthalensis* specimens is comparably thicker. In addition, the *H. sapiens* specimens (except Cro-Magnon 1) display evident thinning of the cerebral fossa of the occipital bone, whereas the *H. neanderthalensis* specimens (except Spy 10) possess a relatively thick cerebral fossa.

Previous research has suggested that thinning of the anterosuperior part of the parietal bone is a prevalent characteristic in both *H. sapiens* and *H. neanderthalensis* and claimed that thinning is associated with compression from the frontal ascending gyri, particularly with the course of the anterior ramus of the middle meningeal system (Balzeau, 2013). Studies of extant human populations have revealed that thinning of the inferior portion of the parietal bone is a common trait in *H. sapiens* (Eisová et al., 2016; Jung et al., 2003; Marsh, 2013). This is also evident in our sample (Figures 1–4). The thinning correspond to the junction between the posterior and uppermost extensions of the temporal gyri and the basal area of the second parietal convolution. The inferior parietal lobule forms a marked relief in our *H. sapiens* specimens

on the endocasts. This relief is directly linked to the observed thinning of the bone in the corresponding area. In contrast, the corresponding area in our sample of *H. neanderthalensis* shows different combinations of features. The Neanderthal inferior parietal lobule forms a less pronounced relief, and the endocast and cranial vault in this area display a more rounded shape than the relatively more vertical orientation observed in *H. sapiens*. Thus, CVT is relatively higher in this area in *H. neanderthalensis* specimens.

Within the relatively thin regions of the frontal bone and the anterosuperior part of the parietal bone, we observe either no DCs or only small and scarce DCs in both samples. The lack of DCs in the corresponding regions may potentially affect communication between DCs and the anterior branch of the middle meningeal vessels. Similarly, the thin areas in the inferior parietal and occipital bones in *H. sapiens* specimens either do not display DCs or only displayed small DC branches, again potentially affecting the communication between the DC and posterior branches of the middle meningeal vessels.

These observations suggest that the different distribution patterns of CVT between hominin samples may contribute to the differences in DC morphology and distribution, possibly influencing the configuration of the cranial circulatory system. However, it is difficult to predict how this morphological variation may affect the functions of the cranial vascular system and brain. As the DC and MMV networks possess extensive anastomoses, even if the drainage pathways are reduced in specific areas, collateral routes can compensate for any potential disruption, thereby maintaining the overall blood circulation within the cranial region.

Future work should expand this study to include more *H. sapiens* and *H. neanderthalensis* fossils to better document the variation within each species, as well as to other human species to identify different characteristics during evolution. However, it is important to pioneer this field by this current study, comparing two closely related species to identify possible differences in the relationship between CVT and DC. This will provide a better understanding of the variation in DCs and the relationship between the skull, cranial circulatory system, and brain. Additionally, while our study focuses on total bone thickness, the three layers of the cranial bone (i.e., the outer table, diploe, and inner table) are not equally thick. Further studies are warranted to estimate the relationship between DCs and the thickness of each layer.

AUTHOR CONTRIBUTIONS

Jiaming Hui: Conceptualization; investigation; writing – original draft; methodology; visualization; writing – review and editing; software; formal analysis. **Antoine Balzeau:**

Conceptualization; funding acquisition; methodology; visualization; writing – review and editing; software; supervision; project administration; resources.

ACKNOWLEDGMENTS

This study was funded by the French National Research Agency (ANR-20-CE27-0009) and China Scholarship Council. Micro-CT data were provided by the French National Museum of Natural History (MNHN), French National Centre for Scientific Research (CNRS), and the Royal Belgian Institute of Natural Sciences (RBINS). We thank Xiujie Wu, Patrick Semal, Ameline Bardo, and Andréa Filippo for their support. We also thank the editors, reviewer Lynn Copes, and an anonymous reviewer for their comments.

FUNDING INFORMATION

China Scholarship Council; Agence Nationale de la Recherche (ANR-20-CE27-0009).

DATA AVAILABILITY STATEMENT

The fossils were curated by the Royal Belgian Institute of Natural Sciences (RBINS) and the Musée de l'Homme, a branch of the French National Museum of Natural History (MNHN). Requests for access to the micro-CT data of Cro-Magnon, Abri-Pataud, La Chapelle-aux-Saints, and La Quina crania can be made on the MNHN website (<http://colhelper.mnhn.fr/>). Requests for access to micro-CT data of Spy crania should be sent to the anthropological collection of the RBINS. The other data (i.e., the DC models and CVT color maps) generated in this study are available upon formal request via email to the corresponding author.

ORCID

Jiaming Hui  <https://orcid.org/0000-0002-5408-0857>

REFERENCES

- Aiello, L., & Dean, C. (1990). *An introduction to human evolutionary anatomy*. Academic Press.
- Balzeau, A. (2007). Variation and characteristics of the cranial vault thickness in the Krapina and Western European Neandertals. *Periodicum Biologorum*, 109(4), 369–377.
- Balzeau, A. (2013). Thickened cranial vault and parasagittal keeling: Correlated traits and autapomorphies of *Homo erectus*? *Journal of Human Evolution*, 64(6), 631–644. <https://doi.org/10.1016/j.jhevol.2013.02.005>
- Balzeau, A., Buck, L. T., Albessard, L., Becam, G., Grimaud-Hervé, D., Rae, T. C., & Stringer, C. B. (2017). The internal cranial anatomy of the middle Pleistocene Broken Hill 1 cranium. *PaleoAnthropology*, 107–138. <https://doi.org/10.4207/PA.2017.ART107>
- Balzeau, A., & Charlier, P. (2016). What do cranial bones of LBI tell us about *Homo floresiensis*? *Journal of Human Evolution*, 93, 12–24. <https://doi.org/10.1016/j.jhevol.2015.12.008>
- Beaudet, A., Carlson, K. J., Clarke, R. J., de Beer, F., Dhaene, J., Heaton, J. L., Pickering, T. R., & Stratford, D. (2018). Cranial vault thickness variation and inner structural organization in the StW 578 hominin cranium from Jacovec cavern, South Africa. *Journal of Human Evolution*, 121, 204–220. <https://doi.org/10.1016/j.jhevol.2018.04.004>
- Breschet, G. (1829). *Recherches anatomiques, physiologiques et pathologiques sur le système veineux*. Villeret.
- Devièse, T., Abrams, G., Hajdinjak, M., Pirson, S., Modica, K. D., Toussaint, M., Fischer, V., Comeskey, D., Spindler, L., Meyer, M., Semal, P., & Higham, T. (2021). Reevaluating the timing of Neanderthal disappearance in Northwest Europe. *Proceedings of the National Academy of Sciences of the United States of America*, 118(12), e2022466118.
- Douka, K., Chiotti, L., Nespoulet, R., & Higham, T. (2020). A refined chronology for the Gravettian sequence of Abri Pataud. *Journal of Human Evolution*, 141, 102730. <https://doi.org/10.1016/j.jhevol.2019.102730>
- Eisová, S., Rangel De Lázaro, G., Pišová, H., Pereira-Pedro, S., & Bruner, E. (2016). Parietal bone thickness and vascular diameters in adult modern humans: A survey on cranial remains. *The Anatomical Record*, 299(7), 888–896. <https://doi.org/10.1002/ar.23348>
- Eisová, S., Velemínský, P., Velemínská, J., & Bruner, E. (2022). Diploic vein morphology in normal and craniosynostotic adult human skulls. *Journal of Morphology*, 283(10), 1318–1336. <https://doi.org/10.1002/jmor.21505>
- Falk, D. (1990). Brain evolution in *Homo*: The “radiator” theory. *Behavioral and Brain Sciences*, 13(2), 333–344. <https://doi.org/10.1017/S0140525X00078973>
- Fedorov, A., Beichel, R., Kalpathy-Cramer, J., Finet, J., Fillion-Robin, J.-C., Pujol, S., Bauer, C., Jennings, D., Fennessy, F., Sonka, M., Buatti, J., Aylward, S., Miller, J. V., Pieper, S., & Kikinis, R. (2012). 3D slicer as an image computing platform for the quantitative imaging network. *Magnetic Resonance Imaging*, 30(9), 1323–1341. <https://doi.org/10.1016/j.mri.2012.05.001>
- García-González, U., Cavalcanti, D. D., Agrawal, A., Gonzalez, L. F., Wallace, R. C., Spetzler, R. F., & Preul, M. C. (2009). The diploic venous system: Surgical anatomy and neurosurgical implications. *Neurosurgical Focus*, 27(5), E2. <https://doi.org/10.3171/2009.8.FOCUS09169>
- Gauld, S. C. (1996). Allometric patterns of cranial bone thickness in fossil hominids. *American Journal of Physical Anthropology*, 100(3), 411–426. [https://doi.org/10.1002/\(SICI\)1096-8644\(199607\)100:3<411::AID-AJPA8>3.0.CO;2-W](https://doi.org/10.1002/(SICI)1096-8644(199607)100:3<411::AID-AJPA8>3.0.CO;2-W)
- Grimaud-Hervé, D. (2002). Endocranial vasculature. In *The human fossil record, brain endocasts—The paleoneurological evidence* (Vol. 3, pp. 273–277). Wiley-Liss.
- Henry-Gambier, D. (2002). Les fossiles de Cro-Magnon (Les Eyzies-de-Tayac, Dordogne): Nouvelles données sur leur position chronologique et leur attribution culturelle. *Paléo*, 14, 201–204. <https://doi.org/10.4000/paleo.1424>
- Hershkovitz, I., Greenwald, C., Rothschild, B. M., Latimer, B., Dutour, O., Jellema, L. M., Wish-Baratz, S., Pap, I., & Leonetti, G. (1999). The elusive diploic veins: Anthropological and anatomical perspective. *American Journal of Physical Anthropology*, 108(3), 345–358. [https://doi.org/10.1002/\(SICI\)1096-8644\(199903\)108:3<345::AID-AJPA9>3.0.CO;2-S](https://doi.org/10.1002/(SICI)1096-8644(199903)108:3<345::AID-AJPA9>3.0.CO;2-S)

- Hui, J., & Balzeau, A. (2023). The diploic venous system in *Homo neanderthalensis* and fossil *Homo sapiens*: A study using high-resolution computed tomography. *American Journal of Biological Anthropology*, 182(3), 412–427. <https://doi.org/10.1002/ajpa.24843>
- Jung, Y.-S., Kim, H.-J., Choi, S.-W., Kang, J.-W., & Cha, I.-H. (2003). Regional thickness of parietal bone in Korean adults. *International Journal of Oral and Maxillofacial Surgery*, 32(6), 638–641. <https://doi.org/10.1054/ijom.2002.0415>
- Kunz, A. R., & Iliadis, C. (2007). Hominid evolution of the arteriovenous system through the cranial base and its relevance for craniosynostosis. *Child's Nervous System*, 23(12), 1367–1377. <https://doi.org/10.1007/s00381-007-0468-5>
- Lachkar, S., Dols, M.-M., Ishak, B., Iwanaga, J., & Tubbs, R. S. (2019). The diploic veins: A comprehensive review with clinical applications. *Cureus*, 11(4), e4422. <https://doi.org/10.7759/cureus.4422>
- Lang, J. (1983). *Clinical anatomy of the head*. Springer. <https://doi.org/10.1007/978-3-642-68242-1>
- Marks, S. C., & Odgren, P. R. (2002). Structure and development of the skeleton. In *Principles of bone biology* (pp. 3–15). Elsevier. <https://doi.org/10.1016/B978-012098652-1.50103-7>
- Marsh, H. E. (2013). *Beyond thick versus thin: Mapping cranial vault thickness patterns in recent Homo sapiens*. Doctor of Philosophy. University of Iowa. <https://doi.org/10.17077/etd.hbxcmbbg>
- Percival, C. J., & Richtsmeier, J. T. (2013). Angiogenesis and intramembranous osteogenesis. *Developmental Dynamics*, 242(8), 909–922. <https://doi.org/10.1002/dvdy.23992>
- Rangel de Lázaro, G., de la Cuétara, J. M., Pišová, H., Lorenzo, C., & Bruner, E. (2016). Diploic vessels and computed tomography: Segmentation and comparison in modern humans and fossil hominids. *American Journal of Physical Anthropology*, 159(2), 313–324. <https://doi.org/10.1002/ajpa.22878>
- Rangel de Lázaro, G., Neubauer, S., Gunz, P., & Bruner, E. (2020). Ontogenetic changes of diploic channels in modern humans. *American Journal of Physical Anthropology*, 173(1), 96–111. <https://doi.org/10.1002/ajpa.24085>
- Raynal, J. P., & Pautrat, Y. (1990). *La Chapelle-aux-Saints et la pré-histoire en Corrèze*. Association pour la recherche archéologique en Limousin.
- Schwartz, J. H., Tattersall, I., & Holloway, R. L. (Eds.). (2002). *The human fossil record, brain endocasts—The paleoneurological evidence* (Vol. 3). Wiley-Liss.
- Semal, P., Rougier, H., Crevecoeur, I., Jungels, C., Flas, D., Hauzeur, A., Maureille, B., Germonpré, M., Bocherens, H., Pirson, S., Cammaert, L., De Clerck, N., Hambucken, A., Higham, T., Toussaint, M., & van der Plicht, J. (2009). New data on the late Neandertals: Direct dating of the Belgian spy fossils. *American Journal of Physical Anthropology*, 138(4), 421–428. <https://doi.org/10.1002/ajpa.20954>
- Tsutsumi, S., Nakamura, M., Tabuchi, T., Yasumoto, Y., & Ito, M. (2013). Calvarial diploic venous channels: An anatomic study using high-resolution magnetic resonance imaging. *Surgical and Radiologic Anatomy*, 35(10), 935–941. <https://doi.org/10.1007/s00276-013-1123-3>
- Tsutsumi, S., Ogino, I., Miyajima, M., Ito, M., Arai, H., & Yasumoto, Y. (2015). Cerebrospinal fluid drainage through the diploic and spinal epidural veins. *Journal of Anatomy*, 227(3), 297–301. <https://doi.org/10.1111/joa.12349>
- Tsutsumi, S., Ogino, I., Miyajima, M., Nakamura, M., Yasumoto, Y., Arai, H., & Ito, M. (2014). Cranial arachnoid protrusions and contiguous diploic veins in CSF drainage. *American Journal of Neuroradiology*, 35(9), 1735–1739. <https://doi.org/10.3174/ajnr.A4007>
- Yamashiro, K., Muto, J., Wakako, A., Murayama, K., Kojima, D., Omi, T., Adachi, K., Hasegawa, M., & Hirose, Y. (2021). Diploic veins as collateral venous pathways in patients with dural venous sinus invasion by meningiomas. *Acta Neurochirurgica*, 163(6), 1687–1696. <https://doi.org/10.1007/s00701-021-04777-4>
- Yu, J., Guo, Y., Xu, B., & Xu, K. (2016). Clinical importance of the middle meningeal artery: A review of the literature. *International Journal of Medical Sciences*, 13(10), 790–799. <https://doi.org/10.7150/ijms.16489>

How to cite this article: Hui, J., & Balzeau, A. (2023). Investigating the relationship between cranial bone thickness and diploic channels: A first comparison between fossil *Homo sapiens* and *Homo neanderthalensis*. *The Anatomical Record*, 1–11. <https://doi.org/10.1002/ar.25360>